Available online at www.sciencedirect.com
ScienceDirect
Ceramics International 33 (2007) 1165–1169
CERAMICS INTERNATIONAL
www.elsevier.com/locate/ceramint

Porosity of freeze-dried γ-Al_2O_3 powders

Carolina Tallón [a], Malcolm Yates [b], Rodrigo Moreno [a], M[a] Isabel Nieto [a,*]

[a] *Instituto de Cerámica y Vidrio, CSIC, C/Kelsen, 5, Cantoblanco, 28049 Madrid, Spain*
[b] *Instituto de Catálisis y Petroleoquímica, CSIC, C/Marie Curie, 2, Cantoblanco, 28049 Madrid, Spain*

Received 29 December 2005; received in revised form 8 February 2006; accepted 14 March 2006
Available online 26 July 2006

Abstract

The porosity, inter-particulate and inter-agglomerate, of γ-Al_2O_3 nanopowders obtained by the freeze-drying method has been studied. Homogeneous spherical granules with diameters ranging from 1 to 100 μm have been obtained. These granules are constituted by soft agglomerates of nanoparticles. The pore volume and size distribution are a function of the freezing kinetics and the processing parameters. Mercury intrusion porosimetry results show that the powders exhibit a multimodal porosity. A mesoporosity with mean size of 10 nm, attributed to the inter-particulate porosity, is practically constant, whereas the inter-agglomerate porosity (100–600 nm), strongly depends on the salt concentration, freezing rate and thermal treatment of the powders.

Keywords: A. Powders: chemical preparation; B. Porosity; D. Al_2O_3

1. Introduction

There is a great interest in porous ceramic materials due to the extensive number of applications in different areas, such as filters for environmental cleanup and reuse, bioreactors, gas or chemical sensors and support materials for catalysts or absorbents. This interest is also extended to the preparation of porous granules for shaping by dry-pressing.

There are a wide variety of synthesis methods to obtain porous materials, including firing ceramic powder compacts with an organic material [1], acid leaching [2,3], ceramic foam preparation [4,5], sol–gel method [6–9] or gelcasting [10–12]. In all these cases, some disadvantages appear, such as being harmful to the environment, applicable to a limited range of materials, low strength final products or a pore structure which cannot be controlled. Porous granules are usually prepared by spray-drying [13–15] or sieve granulation [16] which have also some problems related to the removal of the binder.

In this context, the freeze-drying method has become a useful, versatile, simple and efficient method to obtain porous ceramic materials or granules. It allows control over the porosity by varying a number of parameters and to improve the sinterability of the materials, reducing the temperature of sintering and decreasing the shrinkage and defects [17].

The freeze-drying method [18,19] consists of a rapid freezing in small droplets of a salt solution which contain the desired cation or cations, maintaining the chemical homogeneity. Subsequent sublimation of ice under vacuum conditions leads to porous spheres of the anhydrous salt with a high surface area, which consolidates during the calcination process needed to remove the anion and grow the oxide nanoparticles. The microstructure of the obtained powder shows agglomerates with both porosity between nanoparticles (inter-particulate pores) and between agglomerates (inter-agglomerate pores) [20].

One of the most important ceramic compounds is γ-Al_2O_3 due to its use as adsorbents, catalysts, coatings and soft abrasives [21]. When used as a support in heterogeneous catalysis a high surface area is a fundamental requirement in order to achieve a high dispersion of the catalytically active noble metal or supported oxide species [22,23]. However, to avoid diffusional limitations not only a high surface area but also a highly interconnected open pore structure with a wide range of pores from the nanometre to micro sizes is desirable [24]. Some works have been developed to obtain catalyst supports by freeze-drying method [25–27].

The aim of the present work is to study the influence of different parameters on the porosity and microstructure of alumina powders obtained by a freeze-drying method in terms

* Corresponding author. Tel.: +34 91 7355840; fax: +34 91 7355843.
E-mail address: minieto@icv.csic.es (M.I. Nieto).

0272-8842/$32.00
doi:10.1016/j.ceramint.2006.03.021

of the process parameters, such as solution concentration, rate and temperature of freezing and the calcination temperature.

2. Experimental

The alumina powders were obtained as described in Ref. [28]. The solutions of $Al_2(SO_4)_3{\cdot}18H_2O$ at concentrations of 0.76, 1.00 and 1.40 M were sprayed into the refrigerant (liquid nitrogen or ethanol cooled with an acetone–ice mixture). The frozen solution was freeze-dried and the samples were thermally treated in an air atmosphere at different temperatures (840–1000 °C) for 1 or 2 h to attain γ-alumina. The thermal treatment had intermediate steps at 400 and 840 °C with dwell times of 15 min and 1 h, respectively. The heating rate was 2 °C/min up to 400 °C and 5 °C/min for the other steps.

The specific surface areas were measured by N_2 adsorption at 77 K, by the BET method (Monosorb Surface Area Analyser MS-13, Quantachrome Co., USA), and the porosity by mercury intrusion porosimetry (MIP) (CE Instruments Pascal 140/240, UK). For the latter measurements, the Washburn equation was employed, assuming a non-intersecting cylindrical pore model and the recommended values for the mercury contact angle and surface tension of 141° and 484 mN m^{-1}, respectively [29]. The microstructure was observed using field emission scanning electron microscopy (FE-SEM) (Hitachi S-4700 type I, Japan).

3. Results and discussion

By the freeze-drying method spherical γ-Al_2O_3 nanoparticles are obtained with a primary particle size lower than 20 nm. These nanoparticles arranged into soft and porous agglomerates which form the granules. Fig. 1 shows the cumulative MIP curves obtained for the samples frozen in liquid nitrogen. A multimodal porosity with three well defined regions is observed. A region of mesoporosity (<20 nm), a second interval between 20 and 2–3 μm, and a region corresponding to pores wider than 10 μm. The latter pores cannot be attributed to the true porosity of the samples, as they correspond to the spaces between granules and the partial destruction of the soft agglomerates, due to the applied pressure during the determination. Moreover, no appreciable differences in the intrusion volume or distribution of these pores were observed. Consequently, the results of these last pores are not significant for this study, and further discussion is centred on the interval between 7.5 and 3000 nm, where a bimodal pore size distribution is observed. These measurements agree with the results of Lloyd et al. [30].

The porosimetry data of samples calculated in this way and the surface area results are presented in Table 1. From surface area values, taking measured densities [28], an average primary particle size (d_{BET}) of 13–15 nm was calculated for all the studied samples. No average pore diameter values are presented, because they are not representative due to the multimodal pore size distribution. The porosity of all the samples is higher than 50%, although it decreases when the solution concentration and/or the temperature of thermal treatment are increased, in accordance with the reductions of the surface areas.

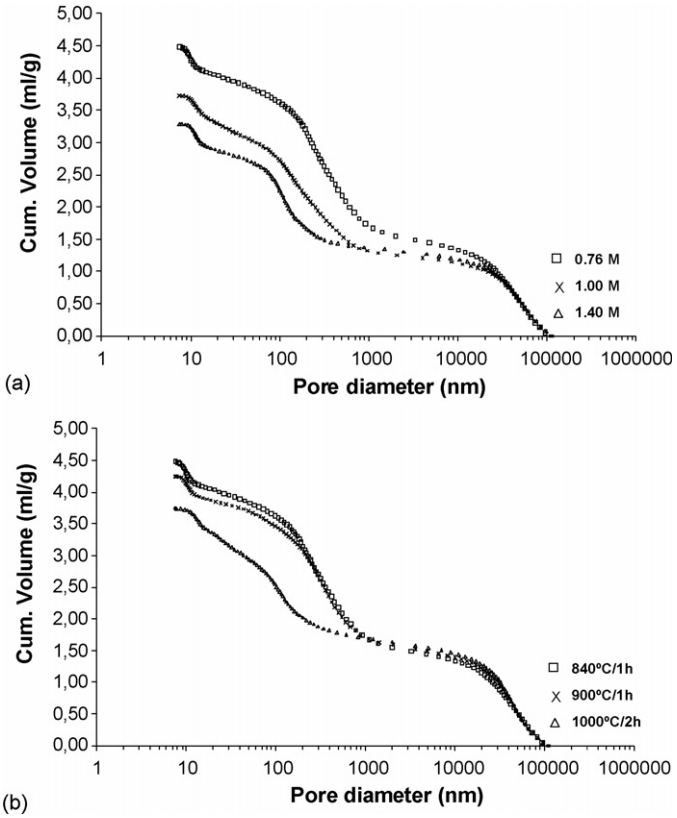

Fig. 1. Cumulative intrusion volume curves of the freeze-dried samples: (a) for different salt solution concentrations and (b) varying the temperature of thermal treatment.

The influence of salt solution concentration on the microstructure of the alumina samples is shown from the pore size distribution curves presented in Fig. 2. As can be observed, the mesoporosity is always located at ≅10 nm, with an intrusion volume of about 0.3 $cm^3\ g^{-1}$ for the three samples. This porosity can be attributed to the inter-particulate porosity, the size of pores and particles was similar and no differences in the distribution or volume of the pores are observed as a function of solution concentration, indicating that the nanostructure of aggregates is similar and no dependant on this concentration.

In Table 2 the corresponding maximum pore diameter and the intrusion volume calculated for the region between 15 and 3 μm are presented. The porosity in this region corresponds to the inter-agglomerate pores. These macropores have different mean size depending on the concentration of the starting

Table 1
Porosity and surface area data of the freeze dried γ-Al_2O_3 particles obtained from solutions with different concentration and thermal treatment

Sample	Sulphate solution (M)	Thermal treatment, *T*/*t* (°C/h)	Intrusion volume[a] ($cm^3\ g^{-1}$)	Porosity[a] (%)	Specific surface area ($m^2\ g^{-1}$)
A1	0.76	900/1	2.57	59	153
A2	1.00	900/1	2.41	60	146
A3	1.40	900/1	1.89	53	146
A4	0.76	840/1	2.87	62	170
A5	0.76	1000/2	1.99	52	127

[a] These data correspond to the interval from 7.5 to 3000 nm.

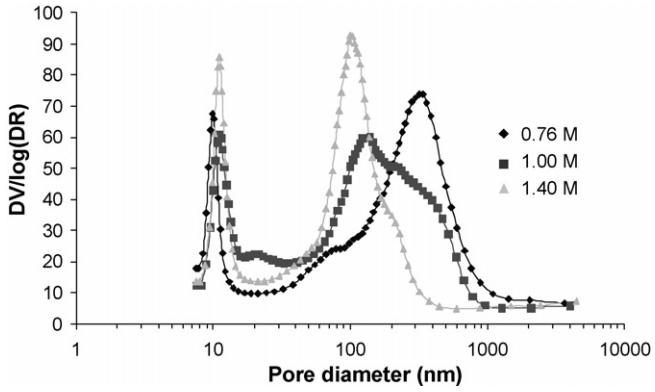

Fig. 2. Pore size distribution curves of samples treated at 900 °C/h as a function of solution concentration from 7.5 to 3000 nm.

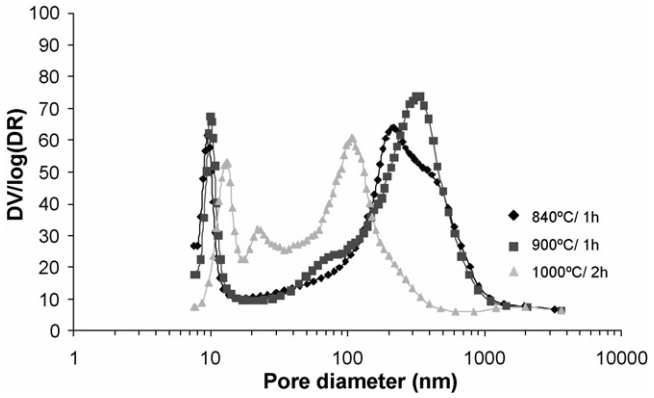

Fig. 3. Pore size distribution curves for 0.76 M samples after different calcination temperatures.

solution, from 320 nm for the 0.76 M solution to 100 nm for the 1.40 M one. For higher concentrations, lower pore diameters and pore volumes are observed. The influence of the salt solution concentration on the porosity is related to its water content [31]: the water freezes forming channels that remain after the sublimation during the freeze-drying process. Consequently, the porosity decreases as the concentration increases due to the lower water content. The different degree of porosity determines the resistance of the aggregates, which increases with the concentration of the solution.

In relation with the thermal treatment, the calcination temperature has a clear influence on the specific surface area (Table 1). Lloyd et al. [32] attribute this phenomenon to the removal of intragranular pores. In addition, the formation of necks in the earlier stages of sintering at 1000 °C is possible. From the analysis of the intrusion and pore size distribution curves (Fig. 3 and Table 2), it can be observed that the total cumulative volume decreases with increasing calcination temperatures, indicating that a more packed agglomerate structure is formed.

In all cases, there is a mesoporosity with a pore volume of 0.3 $cm^3\ g^{-1}$, similar to the data obtained for samples A1–A3. Nevertheless, the maximum diameter of these pores is located at ≅10 nm for the samples thermally treated at 840 and 900 °C, but is wider for the alumina calcined at 1000 °C, and an additional peak in the distribution of pores with a maximum at ≅21 nm appears. When the sintering process starts, the shrinkage produced on the formation of necks leads to an increase of the inter-particulate pores, as observed in the curves of Fig. 3.

Table 2
Intrusion volume and maximum pore diameter data of the freeze dried γ-Al_2O_3 samples in the region of 15 nm–3 μm

Sample	Maximum pore size (nm)	Additional peak or shoulder (nm)	Intrusion volume ($cm^3\ g^{-1}$)
A1	320	70	2.27
A2	130	220	2.11
A3	100	200	1.59
A4	210	400	2.57
A5	105		1.69

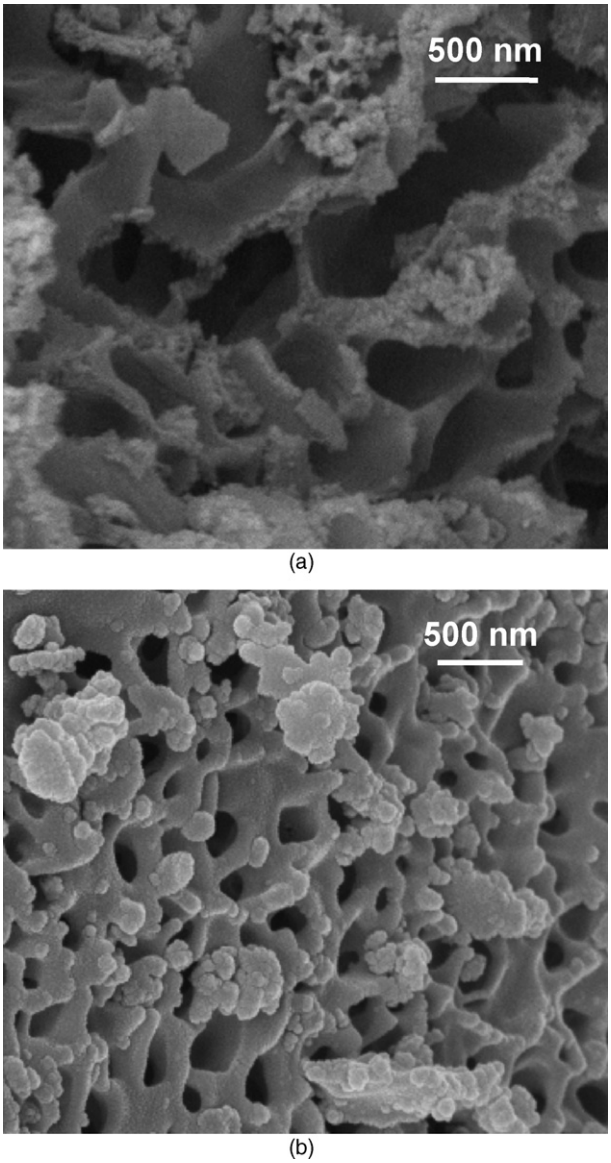

Fig. 4. FE-SEM micrograph of 0.76 M samples treated at: (a) 840 °C/h and (b) 900 °C/h.

The evolution of inter-agglomerate porosity is rather singular. The pore diameter distribution of the sample calcined at 840 °C is wide and shows a maximum at ≅220 nm and a strong shoulder at ≅400 nm, whereas, this distribution for the sample treated at 900 °C is narrower, with a peak at 320 nm. These differences should be associated with an increased crystallinity of the γ-alumina with the treatment temperature and the more homogeneous microstructure formation (Fig. 4). The effect of the beginning of sintering at 1000 °C is more relevant on the inter-agglomerate porosity. It is observed that the maximum of pore diameter largely decreases to 100 nm, as a consequence of the associated shrinkage.

Another parameter with a great influence on the microstructure of freeze-dried alumina is the rate of freezing [17,20]. A refrigerant with very low freezing rate, ethanol cooled with an acetone–ice mixture (−5 °C), was tested and compared to liquid nitrogen (−196 °C). In Fig. 5 the cumulative volume and pore size distribution curves of γ-Al_2O_3 powders obtained by freezing the 0.76 M solution into ethanol and liquid nitrogen (A1) and thermally treated at 900 °C are presented. As with the other parameters studied, no large differences are observed in the mesoporosity inter-particles, only a slightly wider pore size distribution is observed for the sample frozen into ethanol (lower freezing rate).

According to the observed microstructure (Fig. 6), large differences in the inter-agglomerate porosity are detected. The sample frozen at lower rate shows a wider pore size distribution, with a higher maximum (≅550 nm) and a shoulder at ≅2 μm.

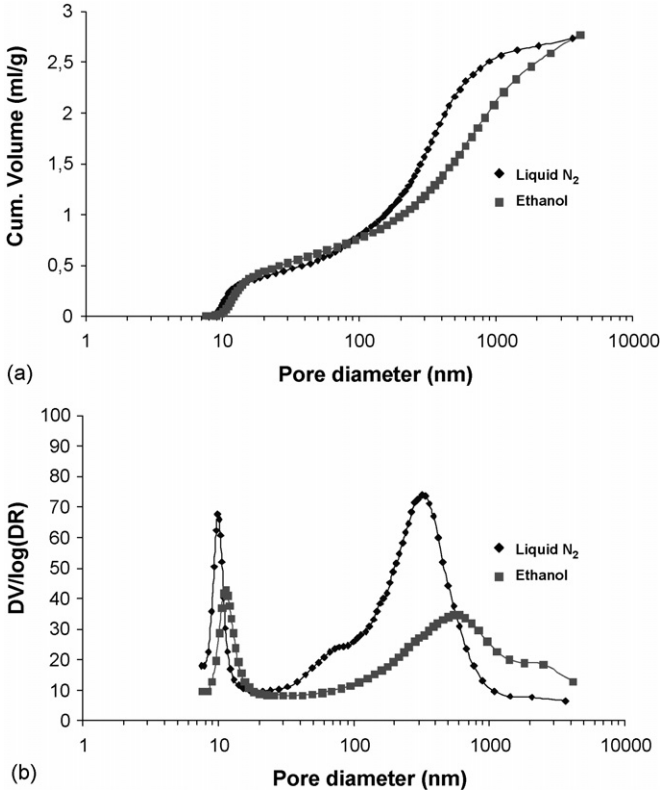

Fig. 5. Curves for 0.76 M samples frozen in different freezing rate refrigerants and calcined at 900 °C/h: (a) cumulative volume curves and (b) pore size distribution curves.

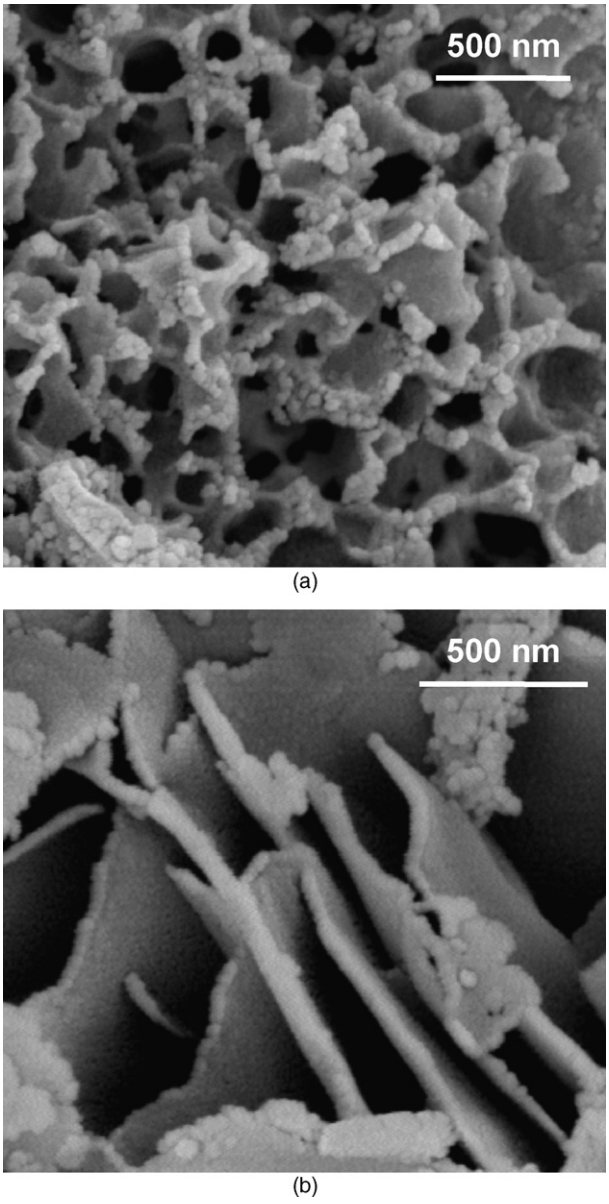

Fig. 6. FE-SEM picture of samples frozen in different refrigerants and treated at 900 °C/h: (a) 1.00 M frozen in liquid nitrogen and (b) 0.76 M frozen in ethanol (cooled with an acetone–ice mixture).

Since, the pore volume is similar (Fig. 5(a)) the number of pores must be lower in the ethanol frozen sample. Consequently, the microstructure of this alumina powder corresponds to bigger agglomerates with larger pores. These data are congruent with the lower surface area for this sample (129 $m^2\ g^{-1}$) and with the freezing process. When the solution is frozen, hydrates which are not soluble in ice are formed, so that salt and water freeze independently [18,32]. If the solution is sprayed over a low freezing rate refrigerant, large ice crystals appear. Both the salt and ice have time enough to grow on different sides of the sample, enhancing the formation of layers of salt without the characteristic channels formed during sublimation of ice in samples frozen in a high freezing rate refrigerant. In the case of samples frozen in ethanol, layers of salt disposed randomly all over the granules without any channels between them are formed,

as can be seen in Fig. 6(b). Samples frozen in liquid nitrogen have a more homogeneous microstructure (Fig. 6(b)) and therefore a more homogeneous pore size distribution than samples frozen in ethanol, where there are larger pores but in lower quantity.

4. Conclusions

The microstructure and characteristics of the nanoparticles of γ-Al_2O_3 obtained by freeze-drying depend on various parameters associated with the process. There are two types of porosity, first, a mesoporosity associated with the inter-particulate pores that is barely influenced by the different parameters involved in the freeze-drying process. In all cases a pore volume of 0.3 $cm^3\ g^{-1}$ and a pore size of $\cong$10 nm, similar to the primary particle size, are obtained. The macroporosity, corresponding to the inter-agglomerate pores, is a function of the process conditions (salt concentration, temperature of calcination and freezing rate). The increase of the salt solution concentration and the temperature of thermal treatment and the decrease of freezing rate produce a decrease in the pore volume. The salt concentration and freezing rate largely influence the pore size distribution, whereas, considering the thermal treatment, the key factor that modifies this pore size is the beginning of the sintering process. Thus, this freeze-drying technique can be used to produce high surface area controlled porosity γ-Al_2O_3 powders that are ideal as catalyst supports.

Acknowledgements

This work has been supported by CICYT (Spain, contract No. MAT2003-836). C. Tallón acknowledges CSIC and ESF for the concession of an I3P-BPD2004 grant. M. Yates gratefully acknowledges the Ramon y Cajal contract X0SC000057.

References

[1] E. Ryshkewitch, Compression strength of porous sintered alumina and zirconia, J. Am. Ceram. Soc. 36 (2) (1953) 65–68.
[2] J. Temuujin, K. Okada, K.J.D. Mackenzie, Preparation of porous silica from vermiculite by selective leaching, Appl. Clay Sci. 22 (2003) 187–195.
[3] A. Makishima, J.D. Mackenzie, J.J. Hammel, The leacing of phase-separated sodium borosilicate glasses, J. Non-Cryst. Solids 31 (1979) 377–383.
[4] A.J. Sherman, R.H. Tuffias, R.B. Kaplan, Refractory ceramic foams: a novel, new high-temperature structure, Am. Ceram. Soc. Bull. 70 (6) (1991) 1025–1029.
[5] F.F. Lange, K.T. Miller, Open-cell, low-density ceramics fabricated from reticulated polymer substrates, Adv. Ceram. Mater. 2 (4) (1987) 827–831.
[6] J.M. Benito, A. Conesa, M.A. Rodríguez, Membranas cerámicas. tipos, métodos de obtención y caracterización, Bol. Soc. Esp. Ceram. V. 43 (5) (2004) 829–842.
[7] R.B. Bagwell, G.L. Messing, Critical factors in the production of sol–gel derived porous alumina, Key Eng. Mater. 115 (1996) 45–64.
[8] L.C. Klein, R.H. Woodman, Porous silica by the sol–gel process, Key Eng. Mater. 115 (1996) 109–124.
[9] S. Sakka, H. Kozuka, T. Adachi, Preparation of Pororus Materials by the Sol–Gel Method, in: K. Ishizaki, L.M. Sheppard, S. Okada, T. Hamasaki, B. Huybrechts (Eds.), Ceramic Transactions, vol. 31, The American Ceramic Society, Westerville, OH, 1993, pp. 27–40.
[10] P. Sepulveda, J.G.P. Binner, Processing of cellular ceramics by foaming and *in situ* polymerisation of organic monomers, J. Eur. Ceram. Soc. 19 (1999) 2059–2066.
[11] R. Mouazer, I. Thijs, S. Mullens, J. Luyten, SiC foams produced by gel casting: synthesis and characterization, Adv. Eng. Mater. 6 (5) (2004) 340–343.
[12] I. Santacruz, M.I. Nieto, R. Moreno, M. Faraldos, E. Sastre, A novel method to prepare zeolite with hierarchical porosity, Adv. Eng. Mater. 7 (9) (2005) 859–861.
[13] N. Uchida, T. Hiranami, S. Tanaka, K. Uematsu, Spray-freeze-dried granules for ceramics fabrication, Am. Ceram. Soc. Bull. 81 (2) (2002) 57–60.
[14] G. Bertrand, C. Filiartre, H. Mahdjoub, A. Foissy, C. Coddet, Influence of slurry characteristics on the morphology of spray-dried alumina powders, J. Eur. Ceram. Soc. 23 (2003) 263–271.
[15] S. Baklouti, T. Chartier, J.F. Baumard, Binder distribution in spray-dried alumina agglomerates, J. Eur. Ceram. Soc. 18 (1998) 2117–2121.
[16] O. Lyckfeldt, K. Rundgren, M. Sjöstedt, Freeze granulation for the processing of silicon nitride ceramics, Key Eng. Mater. 264–268 (2004) 281–284.
[17] T. Fukasawa, Z.-Y. Deng, M. Ando, T. Ohji, Y. Goto, Pore structure of porous ceramics synthesized from water-based slurry by freeze-drying process, J. Mater. Sci. 36 (2001) 2523–2527.
[18] F.J. Schnettler, F.R. Monforte, W.W. Rhodes, A Cryochemical Method for Preparing Ceramics Materials, in: G.H. Stewart (Ed.), Science of Ceramics, The British Ceramic Society, Manchester, United Kingdom, 1968, pp. 79–90.
[19] C. Lacour, M. Paulus, Lyophilisation parameters of ceramic compounds, Sci. Sinter. 11 (3) (1979) 193–202.
[20] I. Haase, R. Müller, Correlation between the powder structure and the microstructure of tetragonal ZrO_2 ceramics, in: P. Durán, J.F. Fernández (Eds.), Third ECERS Proceedings Faenza Editrice Iberica S.L., Castellón de la Plana, Spain, (1993), pp. 727–732.
[21] W.H. Gitzen (Ed.), Alumina as a Ceramic Material, The American Ceramic Society Inc., Columbus, USA, 1970.
[22] J. Blanco, P. Avila, S. Suárez, M. Yates, J.A. Martín, L. Marzo, C. Knapp, CuO/NiO monolithic catalysts for NO_x removal from nitric acid plant flue gas, Chem. Eng. J. 97 (1) (2004) 1–9.
[23] S. Suárez, C. Saiz, M. Yates, J.A. Martín, P. Ávila, J. Blanco, Rh/γ-Al_2O_3-sepiolite monolithic catalysts for decomposition of N_2O traces, Appl. Catal. B Environ. 55 (1) (2004) 57–64.
[24] P. Avila, J. Blanco, J.M.R. Blas, O. Ruiz de los Paños, M. Yates, Sepiolite based monolithic catalysts for the reduction of nitric oxide with propylene in oxidising atmosphere, Stud. Surf. Sci. Catal. 96 (1995) 707–717.
[25] J. Kirchnerova, D. Klvana, Synthesis and characterization of perovskite catalysts, Solid State Ionics 123 (1999) 307–317.
[26] T. Yokota, Y. Takahata, T. Katsuyama, Y. Matsuda, A new technique for preparing ceramics for catalyst support exhibiting high porosity and high heat resistance, Catal. Today 69 (2001) 11–15.
[27] R.X. Valenzuela, G. Bueno, A. Solbes, F. Sapiña, E. Martínez, V. Cortés Corberán, Nanostructured ceria-based catalysts for oxydehydrogenation of ethane with CO_2, Top. Catal. 15 (2–4) (2001) 181–188.
[28] C. Tallón, R. Moreno, M.I. Nieto, Synthesis of γ-Al2O3 nanopowders by freeze-drying, Mater. Res. Bull. 41 (2006) 1520–1529.
[29] J. Rouquerol, D. Avnir, C.W. Fairbridge, D.H. Everett, J.H. Haynes, N. Pericone, J.D.F. Ramsay, K.S.W. Sing, K.K. Unger, Recommendations for the characterization of porous solids, Pure Appl. Chem. 66 (8) (1994) 1739–1758.
[30] I.K. Lloyd, J.R. Blachere, L.A. Beyer, C.E. Kalnas, P.A. Mairet, Characterization of freeze-dried alumina powders using electron microscopy, Ultramicroscopy 29 (1989) 153–160.
[31] J.K.G. Panitz, J.A. Voigt, F.A. Grenlich, M.J. Carr, M.O. Eatough, The morphology of freeze-dried rubidium chloride powder, Mater. Res. Soc. Symp. Proc. 155 (1989) 37–44.
[32] I.K. Lloyd, R.J. Kovel, Pore morphology in cryochemically prepared alumina powders and their sulphate precursors, J. Mater. Sci. 23 (1988) 185–188.